Resolving phase information of the optical local density of state with scattering near-field probes

R. Prasad and R. Vincent*

Laboratoire de Nanotechnologies et d'Instrumentation Optique, ICD, CNRS UMR 6281,
Université de Technologie de Troyes, 12 Rue Marie Curie, 10004 Troyes, France

(Received 5 April 2016; revised manuscript received 29 September 2016; published 25 October 2016)

We theoretically discuss the link between the phase measured using a scattering optical scanning near-field microscopy (s-SNOM) and the local density of optical states (LDOS). A remarkable result is that the LDOS information is directly included in the phase of the probe. Therefore by monitoring the spatial variation of the trans-scattering phase, we locally measure the phase modulation associated with the probe and the optical paths. We demonstrate numerically that a technique involving two-phase imaging of a sample with two different sized tips should allow to obtain the image the pLDOS. For this imaging method, numerical comparison with extinction probe measurement shows crucial qualitative and quantitative improvement.

DOI: 10.1103/PhysRevB.94.165440

I. INTRODUCTION

The rate of spontaneous emission of a fluorescent emitter is determined both by the internal electronic states and the optical local density of state (LDOS) [1]. Luminescence, i.e., the emission of light by a source, can therefore be tailored through the nanostructuration of its environment, thus modifying the LDOS. Due to this tremendous technological impact at the nanoscale, new applications were designed for its development. This is notably true for energy consumption, which allows the enhanced energy extraction for a localized source such as LED [2], OLED [3], and also for an integrated local photon source [4,5], which makes this of a rising interest in the field of telecommunication information for quantum information processing. Thus imaging the LDOS of fabricated samples becomes essential to characterize optical devices, together with a deeper understanding of light-matter interaction. Despite the general interest, such task remains difficult and few works have been reported, which only partially address the question. The main technique developed in the past decade was based on an indirect measurement, typically by determining the life time of a fluorescence emitter [6–8]. However, this kind of optical characterization is mono frequency and remains very dependent on the quality of the source attached to the scan probe microscopy (SPM) and the resolution is still not really convincing. Nevertheless, a relationship between the electromagnetic LDOS and images obtained by optical scanning near-field microscopy (SNOM) have been identified [9,10]. This has been demonstrated experimentally for a well defined near-field structure [11,12]. Despite this, the theoretical approaches that unify LDOS and SNOM images were ultimately neglecting the cross coupling mechanisms between the tip and the structure itself, leading to the introduction of possible errors in the extraction measurements and misleading the interpretations. Recently, taking advantage of the tip-substrate interaction, we have underlined a link between the modification of the width of absorption cross section resonance of a dipolar plasmonic nanoantenna that is in proximity to a given environment and the variation of the corresponding LDOS [13]. However, to go further, i.e., for a quantitative measurement, another approach needs to be considered.

Here, first let us present the considered experimental setup, then some elements on LDOS theory and the polarizability probe, followed by a detail derivation of their connections, and finally we will present the schematic idea behind the LDOS-sensitive technique of the phase. The simulations are based on a discrete dipole approximation (DDA) code that we have used previously to study plasmonic and magneto-optical nanostructures [14].

Since the first development of near-field microscopy [15,16], several types of SNOM have been developed, with different setups and near-field probes. Here, we consider a SNOM operating in the scattering mode with an apertureless dielectric probe and the tip is tilted above the sample, see Fig. 1, in order to realize a measure in transmission.

The incident polarized plane wave E_0 at normal incidence has been focalized on the tip's apex from above and the transmitted light is collected through the sample (see Fig. 1). We will call this configuration trans-scattering SNOM mode (TS-SNOM). The probe's apex is considered to be spherical [17], and vibrates vertically at frequency Ω. Signal demodulation at the tip's oscillation frequency along with an interferometric detection yields transmitted field intensity and phase maps, which corresponds to the local field scattered by the tip, for this we derive formal expressions. Before presenting, the LDOS-sensitive technique of phase (LDOS-SP), let us introduce the theoretical framework that is used to derive the formal expression in this study.

II. THEORY

Assuming the scatterer is small enough to be treated as an electric point dipole [14], the dipole moment $\mathbf{p}$ induced by the exciting local field $\mathbf{E}_{\text{loc}}(\mathbf{r})$, at its position $\mathbf{r}$, is expressed as follows [18]:

$$\mathbf{p}(\mathbf{r},\omega) = \epsilon_0 \boldsymbol{\alpha}(\mathbf{r},\omega)\mathbf{E}_{\text{loc}}(\mathbf{r},\omega) \tag{1}$$

with $\boldsymbol{\alpha}(\mathbf{r},\omega)$ the dressed polarizability [13], that is in the most generalized situation, a tensor, can be written as

$$\boldsymbol{\alpha}(\mathbf{r},\omega) = \frac{\alpha_0}{\boldsymbol{I} - k_0^2 \mathbf{G}_{\text{reg}}(\mathbf{r},\mathbf{r},\omega)\alpha_0} \tag{2}$$

*Corresponding author: remi.vincent@utt.fr

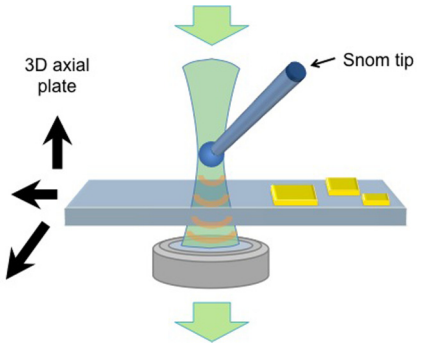

FIG. 1. Trans-scattering-type scanning near-field optical microscopy (TS-SNOM). The wave front illustrates the local field being scattered over the tip and propagating to the detector.

with $\mathbf{G}_{\text{reg}}(\mathbf{r},\mathbf{r}',\omega)$ as the regular part of the electric dyadic Green function. This Green function connects the electric field between two spatial positions and its own information about its environment. $\boldsymbol{I}$ is the identity tensor, the wave number in vacuum is $k_0(=\omega/c=2\pi/\lambda)$, and

$$\alpha_0 = 3V(\epsilon-1)(\epsilon+2)^{-1} \tag{3}$$

is the quasistatic polarizability of the spherical tip's apex of volume V, with the dielectric constant ϵ.

Now, let us recall that the density of the photonics state $\rho(r,\omega)$ is the trace of the imaginary part of the Green function [19], more precisely its regular part $\mathbf{G}_{\text{reg}}(\mathbf{r},\mathbf{r}',\omega)$,

$$\rho(\mathbf{r},\omega) = \frac{6\omega}{\pi c^2}\text{Tr}[\Im[\mathbf{G}_{\text{reg}}(\mathbf{r},\mathbf{r},\omega)]] \tag{4}$$

and the partial LDOS (pLDOS), $\rho_{\mathbf{n}}(r,\omega)$, is a component of this LDOS for a given $\mathbf{n}$ direction. Therefore it can be written as

$$\rho_{\mathbf{n}}(\mathbf{r},\omega) = \frac{6\omega}{\pi c^2}\Im[\mathbf{n}\cdot\mathbf{G}_{\text{reg}}(\mathbf{r},\mathbf{r},\omega)\cdot\mathbf{n}]. \tag{5}$$

It can be noted that the pLDOS is the LDOS available for a point dipole, which is oriented along the direction of $\mathbf{n}$.

III. LDOS-SENSITIVE TECHNIQUE OF PHASE

In our trans-scattering configuration, the vectorial transmitted phase, $\phi_{\text{trans}} = \arg(\mathbf{E}(\mathbf{r}_d,\omega))$, is obtained from the local field that is scattered from the tip and transmitted up to the detector (the direct field being removed by demodulation technique), see Fig. 1. This can be described in terms of the dipolar moment $\mathbf{p}(\mathbf{r},\omega)$, see Eq. (1), propagating up towards the detector (at position $\mathbf{r}_d$)

$$\mathbf{E}(\mathbf{r}_d,\omega) = \mathbf{G}(\mathbf{r}_d,\mathbf{r},\omega)\mathbf{p}(\mathbf{r},\omega). \tag{6}$$

For a general case, the dipolar moment is a combination of moments in several directions depending on the direction of the local field $\mathbf{E}_{\text{loc}} = E_{\text{loc},x}\mathbf{e}_x + E_{\text{loc},y}\mathbf{e}_y + E_{\text{loc},z}\mathbf{e}_z$, and on the polarizability tensor $\boldsymbol{\alpha}(\mathbf{r})$ as given by Eq. (1). Using the following, let us simplify our analysis to the case of layered non gyrotropic substrates (LNGS). Under this condition, the incoming x-polarized plane wave induces a local field polarized along the x-direction $\mathbf{E}_{\text{loc}} = E_{\text{loc}}\mathbf{e}_x$, and the Green function $\mathbf{G}_{\text{reg}}(\mathbf{r},\mathbf{r})$ and $\boldsymbol{\alpha}(\mathbf{r})$ are diagonal. Therefore Eq. (6) can be approximated as follows:

$$\mathbf{E}(\mathbf{r}_d) = \epsilon_0\mathbf{G}(\mathbf{r}_d,\mathbf{r})\mathbf{e}_x[\mathbf{e}_x\cdot\boldsymbol{\alpha}(\mathbf{r})\cdot\mathbf{e}_x]E_{\text{loc}}(\mathbf{r}). \tag{7}$$

This formulation leads to a simple decomposition of the trans-scattered phase, of the transmitted field $\mathbf{E}(\mathbf{r}_d)$ in the direction $\mathbf{e}_x$,

$$\phi_{\text{trans},\mathbf{e}_x} = \arg(\mathbf{E}(\mathbf{r}_d,\omega)\cdot\mathbf{e}_x) = \phi_{G,\mathbf{e}_x} + \phi_{\alpha,\mathbf{e}_x}(\mathbf{r}) + \phi_{E_{\text{loc}}}. \tag{8}$$

In the TS-SNOM mode, the phase in the x direction, $\phi_{\text{trans},\mathbf{e}_x}$, is the sum of the phase of the total Green function $\phi_{G,\mathbf{e}_x} = \mathbf{e}_x\cdot\mathbf{G}(\mathbf{r}_d,\mathbf{r})\cdot\mathbf{e}_x$, in the x direction, that is propagating the field from the probe position up to the detector, the phase of the polarizability tensor in the x-direction $\phi_{\alpha,x}(\mathbf{r},\omega) = \mathbf{e}_x\cdot\arg(\boldsymbol{\alpha}(\mathbf{r},\omega))\cdot\mathbf{e}_x$, and the phase of the local field $\phi_{E_{\text{loc}}}$. This last term $\phi_{E_{\text{loc}}}(\mathbf{r})$, being the usual term, is assumed to be measured in general SNOM interferometric technique. Indeed, the dressed polarizability, Eq. (2), which contains the regular part of the total Green function $\mathbf{G}_{\text{reg}}(\mathbf{r},\mathbf{r},\omega)$, gives the information about the environment.

A. Phase of the near-field probe

Here, let us focus on the second term, the phase of the polarizability in the x-direction $\phi_{\alpha,\mathbf{e}_x}$ and its link to the LDOS in the x direction, $\rho_{\mathbf{e}_x}(\mathbf{r},\omega)$, Eq. (5), and call this quantity, probe's phase shift (PPS). Using Eqs. (2) and (3) along with the probe being dielectric and $Arg(\alpha_0)=0$, the equation can be written as

$$\phi_{\alpha,\mathbf{e}_x}(\mathbf{r},\omega) = \mathbf{e}_x\cdot\arg(\boldsymbol{\alpha}(\mathbf{r},\omega))\cdot\mathbf{e}_x \tag{9}$$

$$= -\mathbf{e}_x\cdot\arg\left(1-k_0^2\boldsymbol{G}_{\text{reg}}(\mathbf{r},\mathbf{r},\omega)\alpha_0(\omega)\right)\cdot\mathbf{e}_x \tag{10}$$

$$= \arctan\frac{k_0^2\alpha_0\Im[\mathbf{e}_x\cdot\mathbf{G}_{\text{reg}}(\mathbf{r},\mathbf{r},\omega)\cdot\mathbf{e}_x]}{1-k_0^2\alpha_0\Re[\mathbf{e}_x\cdot\mathbf{G}_{\text{reg}}(\mathbf{r},\mathbf{r},\omega)\cdot\mathbf{e}_x]}. \tag{11}$$

A direct observation of this formula, informs us that for a small enough value of the quasi-static polarizability α_0 [i.e., small tip, see Eq. (3)], the previous equation (11), gets reduced to the following:

$$\phi_{\alpha,\mathbf{e}_x}(\mathbf{r},\omega) \simeq k_0^2\alpha_0\Im[\mathbf{e}_x\cdot\mathbf{G}_{\text{reg}}(\mathbf{r},\mathbf{r},\omega)\cdot\mathbf{e}_x]. \tag{12}$$

We will see the consequences of this formula in the following sections, where the two cases are explained.

B. In vacuum

It is to be noted that in vacuum $\Im[\mathbf{n}.\mathbf{G}_{\text{reg,vac}}(\mathbf{r},\mathbf{r},\omega).\mathbf{n}] = k_0/6\pi$ and Eqs. (11) and (12) reduce to the following:

$$\phi_{\alpha_{\text{vac}},\mathbf{e}_x} \simeq \arctan\left(\frac{k_0^3\alpha_0}{6\pi}\right) \simeq \frac{k_0^3\alpha_0}{6\pi}. \tag{13}$$

We observe that the probe phase shift is a nonzero value and that it can have consequences in experimental situations. This phenomenon is due to the radiation losses, included in Eq. (2), and is taken into account by the radiation correction in the dipolar polarizability [13], $\alpha_{\text{vac}} = \alpha_0(1-i\frac{k_0^3}{6\pi}\alpha_0)^{-1}$. To illustrate this effect, we have plotted in Fig. 2, its dependence with the probe radius. From this, one can observe the PPS in vacuum has a cubic dependency with the probe's radius, see Eq. (13). It leads to a magnitude of order two proportionality between 25 and 5 nm radius, respectively, and $\phi_{\alpha 25,\mathbf{e}_x} \gg \phi_{\alpha 1,\mathbf{e}_x}$.

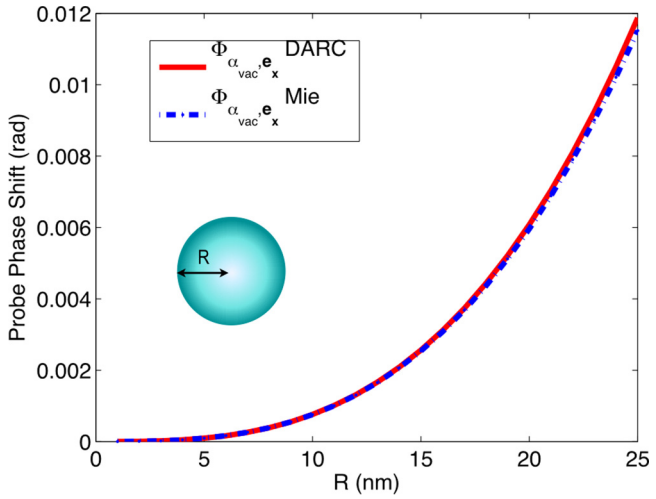

FIG. 2. Vacuum PPS $\phi_{\alpha_{\text{vac}},\mathbf{e}_x}$ in the dipolar approximation with radiative correction (DARC), and with Mie calculation, as a function of the probe's radius.

Let us notice here that a 25-nm dielectric probe creates an intrinsic phase shift of around 0.5°. In Fig. 2, a comparison with Mie theory [20] has been added and it shows that till 25-nm-probe radius the dipolar approach shows small deviation with exact Mie solution.

C. In a given environment

In a general situation of an LNGS, Eq. (12), indicates a remarkable result, the probe's phase shift is proportional to the pLDOS,

$$\phi_{\alpha,\mathbf{e}_x}(\mathbf{r},\omega) \propto \rho_{\mathbf{e}_x}(\mathbf{r},\omega). \tag{14}$$

This is one of the key point of this study. It demonstrates that a measure of the PPS gives us quantitative information about the pLDOS.

Furthermore, using renormalized expressions, we obtain

$$\hat{\phi}_{\alpha,\mathbf{e}_x}(\mathbf{r},\omega) \simeq \frac{6\pi}{k_0}\Im[\mathbf{e}_x \cdot \mathbf{G}_{\text{reg}}(\mathbf{r},\mathbf{r},\omega)\cdot\mathbf{e}_x] = \hat{\rho}_{\mathbf{e}_x}(\mathbf{r},\omega), \tag{15}$$

an equality between the PPS change $\hat{\phi}_{\alpha,\mathbf{e}_x}(\mathbf{r},\omega) = \frac{\phi_{\alpha,\mathbf{e}_x}(r,\omega)}{\phi_{\alpha_{\text{vac}},\mathbf{e}_x}}$ and the LDOS change $\hat{\rho}_{\mathbf{e}_x}(\mathbf{r},\omega) = \frac{\rho_{\mathbf{e}_x}(r,\omega)}{\rho_0(\omega)}$. Normalization is done by dividing the PPS and LDOS by their values in free space, i.e., without the environment $\phi_{\alpha_{\text{vac}},\mathbf{e}_x}$, or equivalently for large distances from the sample.

To illustrate those analytical results, we simulate an experimental configuration that is made up of a silver film of 10-nm thickness. The numerical calculations are realized using a dipole dipole approximation (DDA) code. The impinging light is an s-polarized plane wave at a wavelength of 400 nm, scattering over a spherical particle. The probe is approximated by a dipole [13] and calculations are done at variable distances z above the metallic film. In Fig. 3, we trace the normalized partial LDOS, $\hat{\rho}_{\mathbf{e}_x}(\mathbf{r},\omega)$, the phase of the dipolar moment, $\phi_{p,\mathbf{e}_x} = \arg(\mathbf{p}.\mathbf{e}_x)$, along with the phase of the local field, $\phi_{E_{\text{loc}}}$ and the normalized PPS, $\hat{\phi}_{\alpha,\mathbf{e}_x}$. A 1-nm probe radius is used. The phase of the dipolar moment (PDM) is defined as follows $\phi_{p,\mathbf{e}_x} = \phi_{\alpha,\mathbf{e}_x} + \phi_{E_{\text{loc}}}$.

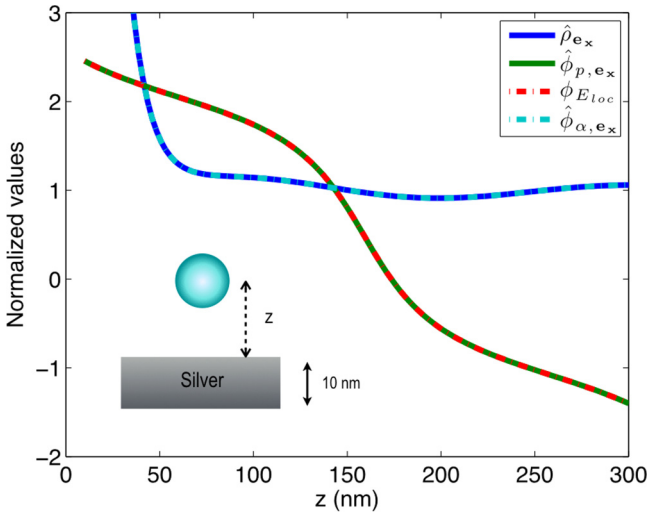

FIG. 3. Normalized partial LDOS $\hat{\rho}_{\mathbf{e}_x}(\mathbf{r},\omega)$, phase of the dipolar moment $\phi_{p,\mathbf{e}_x}$, phase of the local field $\phi_{E_{\text{loc}}}$, and normalized PPS $\hat{\phi}_{\alpha,\mathbf{e}_x}$ at a variable distance of a 10-nm silver film, with a dielectric probe of 1 nm radius, at $\lambda = 400$ nm.

In this case, the PDM and the phase of the local field have very small differences, which are related to the polarizability phase. This illustrates the fact that even in the case of a strong LDOS environment, the PPS remains negligible due to the 1nm probe size. Nevertheless, a comparaison of the normalized PPS with the normalized pLDOS shows a perfect agreement as expected from Eq. (15).

D. Polarizability phase extraction method

Based on the results of the previous sections, a polarizability phase extraction method for pLDOS is proposed, see Fig. 4. After measuring the transmitted phase with tips of different size, and calculating the difference, we obtain the phase

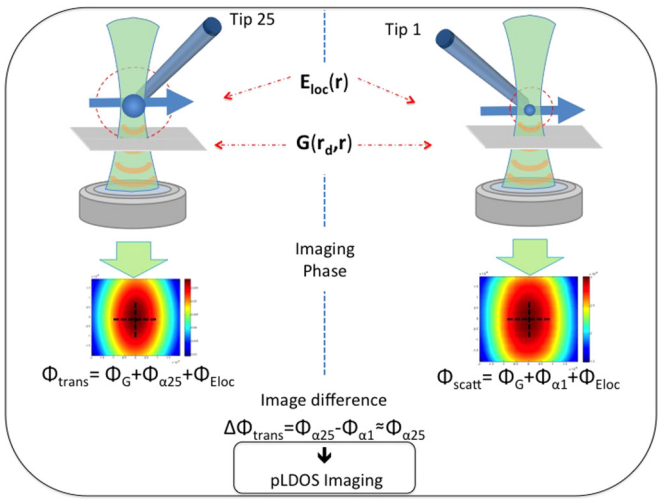

FIG. 4. Illustration of the LDOS phase sensitive (LDOS-SP) technique. It is based on the imaging of the trans-scattering phase map with two different tip sizes that is done sequentially and by normalization of the numerical subtraction, we obtain the map of the pLDOS.

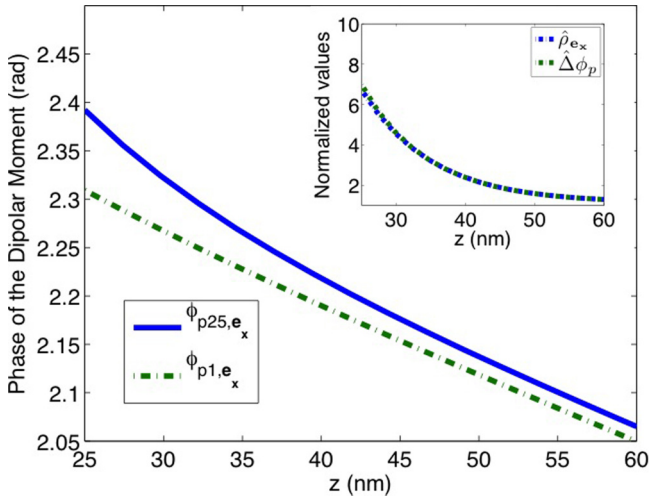

FIG. 5. PDM for two tip radius, $R = 25$ and 1 nm. In insert, normalized pLDOS, and normalized difference of the PDM between the two tip of radius $R = 25$ and 1 nm.

difference of polarizabilities:

$$\phi_{\text{trans25},\mathbf{e}_x} - \phi_{\text{trans1},\mathbf{e}_x} = \phi_{p25,\mathbf{e}_x} - \phi_{p1,\mathbf{e}_x} = \phi_{\alpha 25,\mathbf{e}_x} - \phi_{\alpha 1,\mathbf{e}_x}. \tag{16}$$

Here we assume $\phi_{\alpha 25,\mathbf{e}_x} \gg \phi_{\alpha 1,\mathbf{e}_x}$, based on the previous results, therefore

$$\phi_{\text{trans25},\mathbf{e}_x} - \phi_{\text{trans1},\mathbf{e}_x} \approx \phi_{\alpha 25,\mathbf{e}_x} \propto \rho_{\mathbf{e}_x}(\mathbf{r},\omega). \tag{17}$$

In Fig. 5, the phase of the dipolar moment (PDM) is plotted for two different sizes of the tips, namely, 1 and 25 nm, as a function of the separation distance between the probe and the slab. We observe important phase shift differences between the two tips of up to 0.1 rad ($\simeq 5.5^\circ$) at 25 nm from the surface, revealing strong LDOS effect. Finally, the difference $\Delta\phi_p(z) = \phi_{p25,\mathbf{e}_x} - \phi_{p1,\mathbf{e}_x}$, normalized by its value far from the substrate $\hat{\Delta\phi}_p = \Delta\phi_p(z)/\Delta\phi_p(z \to \infty)$, is plotted in the insert of Fig. 5 and compared to the pLDOS. We find that good adequacies are shown and are in agreement with Eq. (15). In conclusion, simply imaging the trans-scattering phase map with two tip sizes, sequentially would allow us to map the pLDOS by numerical subtraction followed by normalization. In these calculations, a tip of 1-nm radius was considered, but experimentally it is not accessible. The calculation with a radius that is experimentally accessible is of 5 nm, which could be realized as follows: $\phi_{\text{trans25},\mathbf{e}_x} - \phi_{\text{trans5},\mathbf{e}_x} \approx \phi_{\alpha 25,\mathbf{e}_x} \propto \rho_{\mathbf{e}_x}(\mathbf{r},\omega)$. The results are expected to be the same because it is assumed that the PPS, as in the vacuum case, has a cubic dependency with the probe's radius, therefore $\phi_{\alpha 25,\mathbf{e}_x} \gg \phi_{\alpha 5,\mathbf{e}_x} \gg \phi_{\alpha 1,\mathbf{e}_x}$. Finally, as the range of the radius of the tip seems realistic from 5 to 25 nm, the experiment appears to be accessible with the state of the art s-SNOM setup.

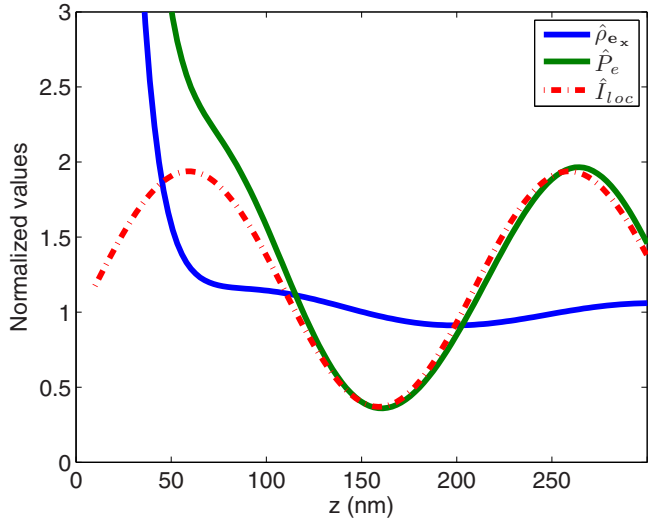

FIG. 6. Normalized extinction, normalized pLDOS, and the normalized local intensity for a 1 nm probe radius at a variable distance of a 10-nm silver film, at $\lambda = 400$ nm.

E. Comparison with extinction

In order to contrast those results with the extinction technique, a simulation based on the same computation code is realized. The extinction measurement is compared with the pLDOS and discrepancies are shown, see Fig. 6. In this figure, we trace the normalized partial LDOS $\hat{\rho}_{\mathbf{e}_x}(\mathbf{r},\omega)$ along with extinction efficiency of the particle $P_e(\mathbf{r},\omega)/P_{e,0}(\mathbf{r},\omega)$ and the local intensity $I_{\text{loc}}(\mathbf{r})$. We can observe a factor of 2 between the pLDOS and the normalized extinction for a distance of around 50 nm from the surface. These differences are due to the intrication of the local field in the extinction response of the particle, the relation at the origin of this effect is demonstrated in the appendix, and given by

$$P_e(\mathbf{r},\omega) = \frac{\omega\epsilon_0}{2V} I_{\text{loc}}(\mathbf{r})[\mathbf{e}_x \text{Im}[\boldsymbol{\alpha}(\omega)] \cdot \mathbf{e}_x]. \tag{18}$$

Aside to this comparison, another remarkable quantity can be resolved, indeed, by dividing the normalized extinction $P_e(\mathbf{r},\omega)/P_{e,0}(\mathbf{r},\omega)$ by the normalized pLDOS $\hat{\rho}_{\mathbf{e}_x}(\mathbf{r},\omega)$ obtained from the LDOS-SP method, we obtain the local intensity $I_{\text{loc}}(\mathbf{r})/I_0$ as follows:

$$\frac{I_{\text{loc}}(\mathbf{r})}{I_0} = \frac{P_e(\mathbf{r},\omega)/P_{e,0}(\mathbf{r},\omega)}{\hat{\rho}_{\mathbf{e}_x}(\mathbf{r},\omega)}. \tag{19}$$

Finally, let us note that the basic idea behind the LDOS-SP method lies in the derived equation (12), which links the PPS and the pLDOS. Therefore any other method that could retrieve the phase of the polarizability would allow us to access the LDOS. For instance, any modulation at the level of the polarizability tensor of the tip (acoustic modulation, anisotropic control, magneto-optic, liquid crystal, etc.) would theoretically allow the same extraction measurement.

IV. CONCLUSIONS

From a theoretical and a numerical analysis point of view, we have confirmed that in an experimental TS-SNOM mode, the extinction and the pLDOS exhibit discrepancies coming from the local field intensity. A framework for the trans-scattering phase of the probe is developed and relationships between the probe's phase shift and the LDOS are established.

These findings have lead us to propose an experimental approach for measuring the LDOS optically and numerical evaluation indicates that it should improve the extinction measurement.

ACKNOWLEDGMENTS

This work was supported by SINPHONIE (ANR-12-NANO-0019) and LABEX ACTION (ANR-11-LABX-01-01) projects funded by Agence Nationale de la Recherche (ANR). Thanks to A. Bruyant for fruitful discussions.

APPENDIX: EXTINCTION BY A NEAR FIELD PROBE

The expression of the dressed polarizability, Eq. (2), can be the starting point to compute the extinction measurement in an arbitrary environment [13]. To carry out this derivation, we start with the expression for the power extracted, i.e., absorbed and scattered, from the external field $\mathbf{E}_{\rm loc}$ by the probe [21]

$$P_e = \frac{1}{2}\int_V Re[\mathbf{j}(\mathbf{r}',\omega)\cdot \mathbf{E}^*_{\rm loc}(\mathbf{r}',\omega)]d^3\mathbf{r}', \tag{A1}$$

where $\mathbf{j}(\mathbf{r}',\omega) = -i\omega\epsilon_0[\epsilon(\omega)-1]\mathbf{E}_{\rm loc}(\mathbf{r}',\omega)$ is the current density induced in the probe. As the electric field is assumed to be uniform inside the probe, and under the assumption of an electrically small probe [13], the extracted power for the probe can be written as

$$P_e = \frac{\omega\epsilon_0}{2V}{\rm Im}[\boldsymbol{\alpha}(\omega)\mathbf{E}_{\rm loc}(\mathbf{r},\omega)\cdot \mathbf{E}^*_{\rm loc}(\mathbf{r},\omega)]. \tag{A2}$$

And using $\mathbf{E}_{\rm loc} = E_{\rm loc}\mathbf{e}_x$, this can be rewritten as

$$P_e(\mathbf{r},\omega) = \frac{\omega\epsilon_0}{2V} I_{\rm loc}(\mathbf{r})[\mathbf{e}_x {\rm Im}[\boldsymbol{\alpha}(\omega)]\cdot\mathbf{e}_x]. \tag{A3}$$

This expression connects the extinction measurement with a cross product between the electric field and a term related to the imaginary part of the polarizability of the probe's tip.

[1] W. L. Barnes, J. Mod. Opt. **45**, 661 (1998).
[2] J. J. Wierer, Jr., A. David, and M. M. Megens, Nat. Photon. **3**, 163 (2009).
[3] K. Saxenaa, V. K. Jaina, and D. S. Mehtab, Opt. Mater. **32**, 221 (2009).
[4] T. Schröder, A. W. Schell, G. Kewes, T. Aichele, and O. Benson, Nano Lett. **11**, 198 (2011).
[5] A. Laucht, S. Pütz, T. Günthner, N. Hauke, R. Saive, S. Frédérick, M. Bichler, M.-C. Amann, A. W. Holleitner, M. Kaniber, and J. J. Finley, Phys. Rev. X **2**, 011014 (2012).
[6] D. Cao, A. Cazé, M. Calabrese, R. Pierrat, N. Bardou, S. Collin, R. Carminati, V. Krachmalnicoff, and Y. De Wilde, ACS Photon. **2**, 189 (2015).
[7] M. Frimmer, Y. Chen, and A. F. Koenderink, Phys. Rev. Lett. **107**, 123602 (2011).
[8] A. W. Schell, P. Engel, J. F. M. Werra, C. Wolff, K. Busch, and O. Benson, Nano Lett. **14**, 2623 (2014).
[9] R. Carminati and J. J. Sáenz, Phys. Rev. Lett. **84**, 5156 (2000).
[10] G. Colas des Francs, C. Girard, J. C. Weeber, and A. Dereux, Chem. Phys. Lett. **345**, 512 (2001).
[11] C. Chicanne, T. David, R. Quidant, J. C. Weeber, Y. Lacroute, E. Bourillot, A. Dereux, G. Colas des Francs, and C. Girard, Phys. Rev. Lett. **88**, 097402 (2002).
[12] C. Huang, A. Bouhelier, G. Colas Des Francs, G. Legay, J. C. Weeber, and A. Dereux, Opt. Lett. **33**, 300 (2008).
[13] E. Castanie, R. Vincent, R. Pierrat, and R. Carminati, Intern. J. Opt. **2012**, 452047 (2012).
[14] R. Vincent, H. Marinchio, J. J. Saenz, and R. Carminati, Phys. Rev. B **90**, 241412(R) (2014).
[15] A. Lewis, M. Isaacson, A. Harootunian, and A. Muray, Ultramicroscopy **13**, 227 (1984).
[16] D. W. Pohl, W. Denk, and M. Lanz, Appl. Phys. Lett. **44**, 651 (1984).
[17] Y. Oshikane, T. Kataoka, M. Okuda, S. Hara, H. Inoue, and M. Nakano, Sci. Technol. Adv. Mater. **8**, 181 (2007).
[18] G. Colas des Francs, S. Derom, R. Vincent, A. Bouhelier and A. Dereux, Int. J. Opt. **2012**, 175162 (2012).
[19] R. Carminati, A. Cazé, D. Cao, F. Peragut, V. Krachmalnicoff, R. Pierrat, and Y. De Wilde, Surf. Sci. Rep. **70**, 1 (2015).
[20] G. Mie, Ann. Phys. **330**, 377 (1908).
[21] S. Albaladejo *et al.*, Opt. Express **18**, 3556 (2010).